SHRESTHA, S. C.
R and M Consultants, Inc., Irvine, California, U.S.A.
BELL, J. R.
Oregon State University, Corvallis, Oregon, U.S.A.

Creep Behavior of Geotextiles Under Sustained Loads

Le fluage des géotextiles sous charges permanentes

Selection of design tensile stress and tensile strain of geotextiles depends upon their time dependent behavior under sustained (static) and/or repetitive (dynamic) loading conditions. Creep of six typical geotextiles under static loads was investigated to develop their creep parameters using an analogy of a four-element rheological model based on Rate Process Theory, and by using an empirical three-parameter creep equation based on curve-fitting of the laboratory data. The parameters were then used to predict the long-term creep behaviors of the six geotextiles. Both methods predicted the time required to reach failure strains as being much shorter than the normal design lives of geotextiles uses at stress level as low as thirty percent of the ultimate. The creep strain-time relationships predicted by the Rate Process Theory appeared to be more consistent with the experimental data than those predicted by the empirical method.

Le choix, pour les géotextiles, d'une contrainte de tension admissible et de leur allongement correspondant, depend de leur comportement qui est fonction du temps, sous les deux conditions de chargement suivantes: charge permanente (cas statique) et charge cyclique (cas dynamique). Le fluage de six géotextiles types sous charge statique a ete étudié afin de trouver les paramètres de fluage; un modèle rhéologique à quatre elements fondé sur la théorie du "Rate Process" a été utilisé ainsi qu'une équation empirique à trois variables obtenue à partir d'une courbe tracée suivant les resultats de laboratoire. Ces deux méthodes ont montré que le temps nécessaire pour obtenir des deformations à la rupture, est beaucoup plus court que la durée de vie admissible des géotextiles soumis à des niveaux de contraintes aussi bas que 30% de celui de la rupture. Les relations de fluage, entre déformation et temps, que l'on a établies à partir de la théorie du "Rate Process" paraissent d'avantage compatible avec les résultats obtenus par expérience qu'avec ceux obtenus par la méthode empirique.

INTRODUCTION

The time-dependent tensile stress-strain behavior of geotextiles under sustained and/or repetitive loads are important for their satisfactory performance in civil engineering applications. For example, an earth wall reinforced with geotextile may fail by excessive deformation due to the unchecked creep of the geotextile even though adequate factors of safety are provided against reinforcement rupture and pullout (1). Similarly, in a road stabilization application, failure may occur due to excessive deformation of the road embankment as a result of excessive creep in the geotextile. If the dead load is much greater than the live load, such as under a thick road embankment, the static creep would be more important in controlling the deformation. However, if the live load is greater than the dead load, such as under a thin road embankment, the dynamic creep would be more important than the static creep in controlling the deformation (2). The design tensile load and tensile strain selected for applications such as these would depend upon the static and/or dynamic creep characteristics of the geotextiles.

There have been attempts by engineers and researchers to characterized the static creep behavior of geotextiles by using simple rheological models and curve-fit methods. Nevertheless, there is a need for a means of not only relating the sustained load and creep strain, but also of predicting the behavior of geotextiles that is based on a rational, analytical theory. One theory which has the potential of fulfilling this need is the Rate Process Theory.

The purpose of this paper is to describe a laboratory investigation to determine the validity of the Rate Process Theory in predicting the tensile creep behavior of geotextiles under sustained load. The observed creep behavior was analyzed by using an analogy of a four-element rheological model whose spring and dashpot constants were determined on the basis of the Rate Process Theory. The creep data were also analyzed on the basis of a curve-fit method which results in a three-parameter phenomenological equation similar to the one used for soils by Singh and Mitchell (3). The parameters developed from the analyses were then used to predict the time for the geotextiles to reach their failure strains under sustained load.

CREEP AS A RATE PROCESS

The Rate Process Theory formulated originally by Eyring (4) has had wide applications in recent years to many processes involving time-dependent rearrangement of matter such as the deformation of materials under stress. M. Hogan (5) used this theory to investigate the creep characteristics of several plastic laminae and it was found to be a highly satisfactory engineering hypothesis applicable to that particular material.

Herrin and Jones (6) and Hady and Herrin (7) used this theory to describe the shear-deformation and creep characteristics of bituminous materials. They found that the behavior of asphalt seemed to be satisfactorily explained by the theoretical considerations suggested by the Rate Process Theory. This theory has also been successfully used by several investigators to describe the creep and consolidation behavior of soils under stress (8,9,10).

Coleman and Knox (11) observed in their theoretical

analysis of the strength properties of textile fibers that it may be possible to predict the stress-strain-time behavior of some textile fibers under both instances of static and dynamic loading by using the Rate Process Theory.

The details of the derivation of the theory is not presented in this paper due to limitation of space. The basis of the relationship is that the atoms and molecules participating in a deformation process are constrained from movement relative to each other by virtue of the energy barriers separating equilibrium positions as shown schematically by Curve A in Figure 1(a). When an external force is applied to the system, flow of the material occurs and it is assumed that the flow takes place by the movement of atoms, molecules or aggregates of molecules (called flow units) into vacancies in the material, or by displacement of the vacancies themselves within the material (6). The displacements of flow units to new positions require that they become "activated" through acquisition of sufficient energy, ΔF, known as the free energy of activation, to surmount the energy barrier.

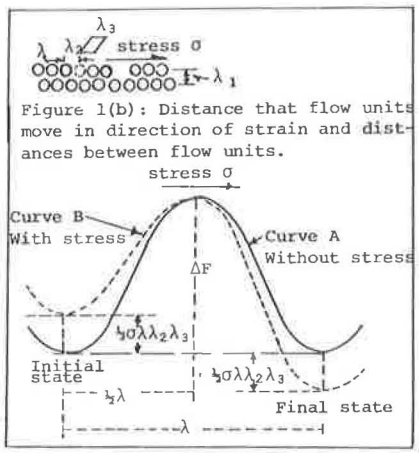

Figure 1 (a): Energy barriers for strain with and without external applied stress

It is assumed in this theory that the flow units are arranged as shown in Figure 1(b). From statistical mechanics, it is known that the flow units in fact are not at rest but vibrate with a frequency of kT/h, as a consequence of their thermal energy, and the specific rate of process is given by Eq. 1 (4).

$$K_r = \frac{kT}{H} e^{\frac{-\Delta F}{RT}} \qquad (1)$$

where: K_r = specific frequency of activation
k = Boltzmann's constant (1.38×10^{-16} erg $^{\circ}K^{-1}$)
h = Planck's constant (6.624×10^{-27} erg sec $^{-1}$)
T = absolute temperature, $^{\circ}K$
R = the universal gas constant = 1.98 cal $^{\circ}K^{-1}$ mole $^{-1}$
ΔF = free energy of activation.

When an external energy is added to the system on application of a force, the original energy barrier becomes distorted as shown by Curve B in Figure 1(a), such that the energy barrier height is reduced in the direction of force and raised the same amount in the direction opposite to the force. Eyring, et al. (4) examined the nature of this phenomenon at considerable length and obtained for the rate of strain the following relationship.

$$\dot{\varepsilon} = 2 \frac{V_h}{V_d} \left(\frac{kT}{h} e^{-\frac{\Delta F}{RT}}\right) \sin h \frac{V_h}{2kT} \sigma \qquad (2)$$

where: $\dot{\varepsilon}$ = the rate of strain
σ = applied stress
$V_h = \lambda_1\lambda_2\lambda_3$ = flow volume of a flow unit
$V_d = \lambda\lambda_2\lambda_3$ = volume of a flow unit
λ = distance the flow units move in the direction of strain
$\lambda_2\lambda_3$ = the cross sectional area of the flow units
λ_1 = distance between flow units.

When a material is subjected to a constant tensile stress of sufficient magnitude the material undergoes a continuous deformation with the passage of time. If the unit strain observed for the body is plotted as ordinate and time as abscissa there is obtained, in general, a curve of the form shown in Figure 2(a). On application of the stress, σ, an instantaneous deformation, ε_o, occurs which remains constant with time, see Figure 2(b).

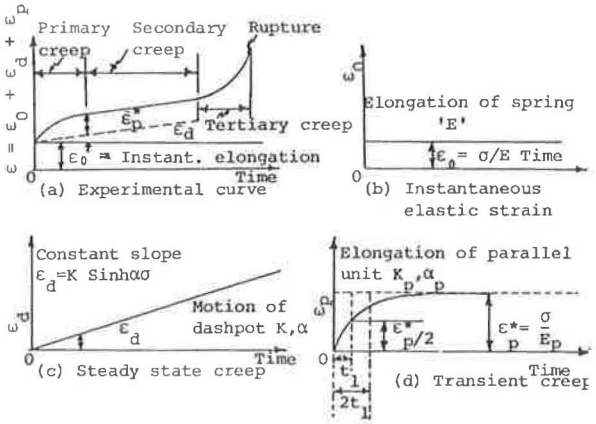

Figure 2: Illustration of creep

With the elapse of time, deformation continues with variable and constant rates, simultaneously. The variable rate of deformation is referred to as the "transient creep component" and the constant rate of deformation is known as the "secondary creep component" of the creep action. These are represented in Figures 2(d) and 2(c), respectively. Following the secondary creep is another phase which is commonly referred to as the "tertiary creep". Tertiary creep occurs at a rapidly increasing rate and eventually leads to failure by rupture.

Engineering interest in the creep properties of a material is largely in that sustained period of time, known as the secondary creep range, during which the creep rate is practically constant (5). Since no engineering use could be made of a material that is in a process of failure, the nature of the tertiary creep is not of any engineering interest. However, the stress level and time at which it develops must be predicted so that it can be avoided.

The creep of a material can be conveniently analyzed by using an analogy of the four-element mechanical model shown in Figure 3. The instantaneous deformation, on application of the load, is represented in the model by the elastic spring E. This constant deformation is graphically represented by Figure 2(b). The transient creep component is represented in the model by the unit consisting of the spring E_p and the dashpot K_p, α_p in parallel. The secondary creep component is represented by the open dashpot K, α.

Of the two constants K and α of the viscous element, K specifies the rate of flow of the dashpot and is expressed in reciprocal seconds and the constant α denotes

the resistance of the element to external force and has

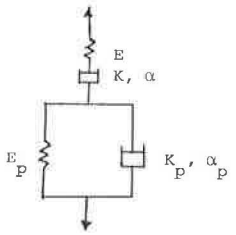

Figure 3: Burger Model.

the units of reciprocal of stress. The point to be noted is that in most rheological models, the viscous element is represented by a single constant known as the viscosity. However, in the rheological model used in this analysis, the viscous element is represented by two constants K and α whose values are determined by the use of the Rate Process Theory. The advantage of this is that the nonlinearity of the viscous element can be represented as subsequently discussed.

Let E be the spring modulus of the open spring (which is the usual modulus of elasticity of fabrics obtained by static loading) and E_p represent the like property of the parallel spring. Furthermore, let σ be the stress applied to the four-element model and σ_d be the stress acting on the parallel viscous element than $(\sigma-\sigma_d)$ will be the stress acting on the parallel elastic element. When the stress σ is applied, the open elastic element E experiences an instantaneous strain ε_o which is given by

$$\varepsilon_o = \frac{\sigma}{E} \tag{3}$$

With the elapse of time, the open viscous element slips at a rate of flow which is given by Eq. 4 derived from the Rate Process Theory.

$$\frac{d\varepsilon_d}{dt} = \dot{\varepsilon}_d = K \sinh \alpha\sigma \tag{4}$$

where: ε_d = strain in the open viscous element

$K = 2 \frac{V_h}{V_d} \frac{kT}{h} e^{-\Delta F/RT}$

$\alpha = V_h/2kT$

t = time.

The steady-state condition of the two open elements subjected to constant stress is given by Eqs. 3 and 4.

The two parallel units representing the transient component of creep deformation each experience the same unit strain at any moment. That is,

$$\frac{d\varepsilon_p}{dt} = \dot{\varepsilon}_p = \frac{1}{E_p} \frac{d(\sigma-\sigma_d)}{dt} = K_p \sinh \alpha_p \sigma_d \tag{5}$$

where: ε_p = creep strain of the parallel elements

$K_p = 2 \frac{V_{hp}}{V_{dp}} \frac{kT}{h} e^{-\Delta F/RT}$

$\alpha_p = \frac{V_{hp}}{2kT}$

From Eq. 5, the following relationships can be derived

$$E_p = \frac{\sigma}{\varepsilon_p^*} \tag{6}$$

$$\ln \frac{\tanh \frac{\alpha_p \sigma}{2} \left(1 - \frac{\varepsilon_p}{\varepsilon_p^*}\right)}{\tanh \frac{\alpha_p \sigma}{2}} = K_p E_p \alpha_p t \tag{7}$$

where: ε_p^* = transient creep at t = infinity.

Equation 7 expresses the variation of the transient creep strain ε_p as a function of time for a constant stress σ. Then, the total strain at any time t, due to a constant stress σ, is given by the sum

$$\varepsilon = \varepsilon_o + \varepsilon_d + \varepsilon_p \tag{8}$$

THREE-PARAMETER CREEP THEORY

Singh and Mitchell (3) found the simple phenomenological equation derived from creep data to hold for creep behavior of a variety of clays. The data obtained from constant stress creep tests of the clays were plotted as shown in Figure 4 and the following creep equation was derived from the slopes of these plots:

$$\dot{\varepsilon}_{(t,\sigma)} = A\, e^{\bar{\alpha}\bar{\sigma}} \left(\frac{t_1}{t}\right)^m \tag{9}$$

for $t_1 = 1$, Eq. 9 reduces to

$$\dot{\varepsilon}_{(t_1,\sigma)} = A\, e^{\bar{\alpha}\bar{\sigma}} \cdot \frac{1}{t^m} \tag{10}$$

where: $\dot{\varepsilon}_{(t,\sigma)}$ = strain rate at time t and deviator stress σ

$\bar{\sigma}$ = ratio of deviator stress of interest to maximum deviator stress

t = time

$m, \bar{\alpha}, A$ = experimentally obtained constants.

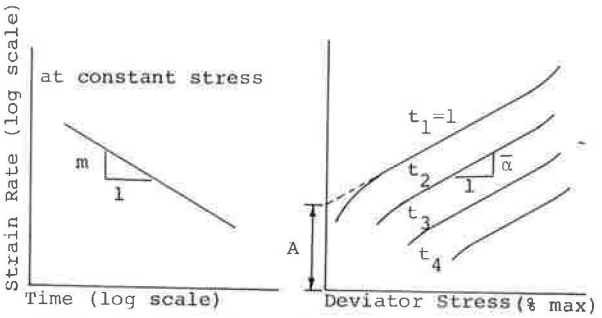

Figure 4 : Method of plotting creep data to empirically determine the constants m, $\bar{\alpha}$, A for three-parameter creep equations. After Singh and Mitchell

Integrating Eq. 10 within the time limit $t = t_1 = 1$ to any time t, creep strain can be expressed as:

$$\varepsilon = \varepsilon_1 + \frac{A}{1-m} e^{\bar{\alpha}\bar{\sigma}} (t^{1-m} - 1) \quad \text{for } m \neq 1 \tag{11}$$

$$\varepsilon = \varepsilon_1 + A\, e^{\bar{\alpha}\bar{\sigma}} \ln t \quad \text{for } m = 1 \tag{12}$$

where ε_1 = creep strain at unit time.

Singh and Mitchell (3) proposed these relationships for creep stresses from 30% to 90% of the initial soil strength, depending upon the susceptibility of the soil to fail in creep rupture (tertiary creep). Note that $\bar{\alpha}$ cannot have negative values, because negative values of $\bar{\alpha}$ would imply that creep strain rate and creep strain are both lower for higher stresses; this phenomenon would be opposite of the normal creep behavior of both soils and geotextiles.

APPARATUS AND EXPERIMENTAL PROCEDURE

The apparatus used for experimental work was a MTS closed-loop testing machine, automatic load and elongation (x-y)

recorder, and special fabric clamps consisting of 229 mm (9 inches) wide by 57 mm (2-1/4 inches) high jaws with serrated faces.

Specimen size used for the creep tests were 200 mm (8 inches) wide by 100 mm (4 inches) initial gauge length. The specimen was installed in the two special jaws mounted in the tensile test machine, and a predetermined tensile load applied under a load-controlled mode. The load was applied by a ramp function such that the desired load was reached in 0.5 seconds and held constant thereafter until the end of the test. The initial and the creep displacement were measured on the x-y recorder. The load and displacements were checked regularly by a digital voltmeter and a measuring scale respectively to check the displacements recorded on the x-y recorder.

The sustained load and the load level used on the four nonwoven and two woven geotextiles selected for the test are presented in Table 1. A total of 12 creep tests consisting of two stress levels for each of six geotextiles were performed.

Table 1. Stress Levels for Creep Tests

Fabric	Geotextile Construction	Filament	Sustained Load N/cm (lbs/inch)	Load Level* %
NW-1	Nonwoven, Resin bonded	Polyester, Continuous	32 (18) 44 (25)	40 57
NW-3	Nonwoven, Heat bonded	Polypropylene, Continuous	47 (27) 86 (49)	35 63
NW-5	Nonwoven, Needlepunched	Polypropylene, Continuous	0.11 (2.2)+ 0.20 (3.8)+	37 57
NW-6	Nonwoven Needlepunched	Polypropylene, Staple	26 (15) 46 (26)	33 56
W-4	Woven	Polypropylene, Monfilament	126 (72) 180 (103)	31 44
C-1	Woven, with Needled Nap	Polypropylene, Slit Film	77 (44) 117 (67)	36 55

*Stress level is the sustained stress as % of the maximum strength.

+Stress normalized to weight per unit area in $\frac{N/cm}{gm/m^2}$ ($\frac{lbs/inch}{oz/yd^2}$).

The laboratory room temperature and humidity were 68° to 82°F and 20% to 58% respectively.

RESULTS

Table 2 shows the creep of the six geotextiles tested for 20 hours under constant stress. Lowest creep was exhibited by polyester resin bonded NW-1 and the highest creep was exhibited by polypropylene needlepunched NW-6. Creep was most sensitive to load levels for the continuous filaments polypropylene geotextiles, NW-3 and NW-5, which showed increased creep of 3 to 5 times when the sustained load was doubled. For NW-1 which was polyester and NW-6 which had staple filaments, creep increased by only 1% to 2% for increase in the sustained load levels from 50% to 57% and 33% to 56% respectively. The woven W-4 and C-1 had lower creep than most nonwovens.

Table 3 presents the constants for the three-parameter creep equation developed from the creep data. The values of m did not differ greatly from one fabric type to another. Greatest variation was found in the values of A with lowest values for NW-1 and highest for NW-6 which had the lowest and the highest creep strains respectively. The values of the constant $\bar{\alpha}$ were all positive.

Table 2. Creep of Geotextiles

Fabric	Creep Measured in 20 Hours: Load Level %	Creep %	Load Level %	Creep %
NW-1	40	3	57	4
NW-3	35	5	63	27
NW-5	33	9	57	31
NW-6	33	20	56	22
W-4	31	11	44	16
C-1	36	5	55	8

Table 3. Constants for Three-Parameter Creep Equation

Fabric	m	A %/minute	$\bar{\alpha}$
NW-1	0.62	0.01	3.59
NW-3	0.74	0.13	2.99
NW-5	0.61	0.06	4.67
NW-6	0.84	0.85	1.23
W-4	0.73	0.29	2.15
C-1	0.73	0.20	1.18

Table 4 gives the constants for creep of geotextiles from Rate Process Theory. The constant E represents the static modulus instantaneously after application of the stress. The magnitude of transient creep depends upon the constant E_p and the steady-state creep depends upon the constants K and α.

Table 4. Constants for Creep of Fabrics by Rate Process Theory

Fabric	K_p 1/second	α_p m/kN	E_p kN/m	K 1/second	α m/kN	E kN/m
NW-1	11×10^{-7}	0.74	173	5×10^{-8}	0.42	66
NW-3	8×10^{-7}	1.03	109	3×10^{-8}	0.60	116
NW-5	61×10^{-7}	0.02*	1.8*	10×10^{-8}	0.01*	0.6*
NW-6	5×10^{-7}	2.51	22	53×10^{-8}	0.23	21
W-4	15×10^{-7}	0.40	198	29×10^{-8}	0.11	182
C-1	18×10^{-7}	0.34	240	35×10^{-8}	0.08	163

*Normalized to gm/m^2.

Figures 5 to 10 show comparisons of the experimental creep curves and those determined by the three-parameter creep equation and by the Rate Process Theory. The creep curves determined by the Rate Process Theory appear to be more consistent with the experimental curves.

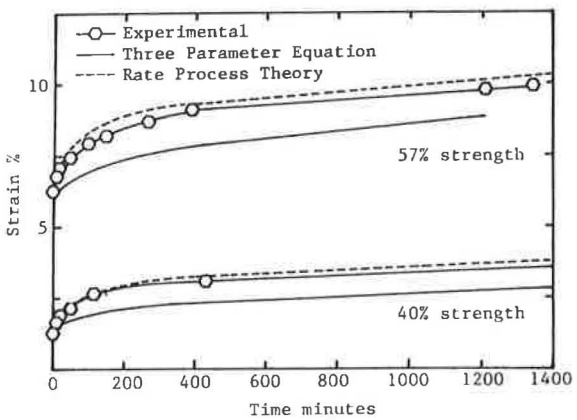

FIGURE 5 : Creep strain vs. time for NW-1 fabric

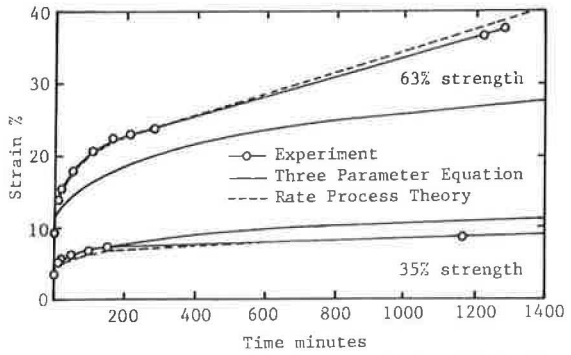

FIGURE 6: Creep strain vs. time for NW-3 fabric

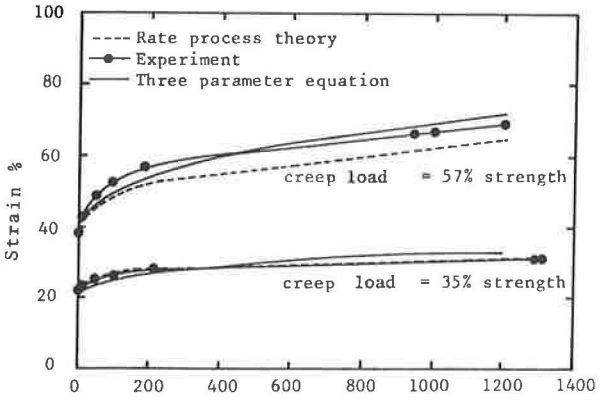

Figure 7: Creep strain vs time for a Fabric NW-5.

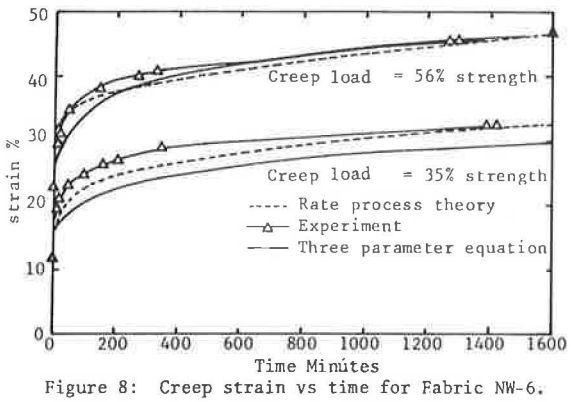

Figure 8: Creep strain vs time for Fabric NW-6.

ANALYSIS OF RESULTS

The basic difference between the three-parameter creep equation and the creep equation derived from Rate Process Theory is that in the former the strain rate is considered as continuously decreasing with passage of time; and in the latter the creep rate is considered as continuously decreasing during the transient stage until a minimum value is reached, and then remains constant at this minimum value during the secondary stage until the beginning of the tertiary creep. During tertiary creep, strain rate increases very rapidly and failure occurs by rupture.

On the basis of the creep parameters presented in Tables 3 and 4, lengths of time at which the geotextile would creep to given strains can be calculated. Table 5 shows

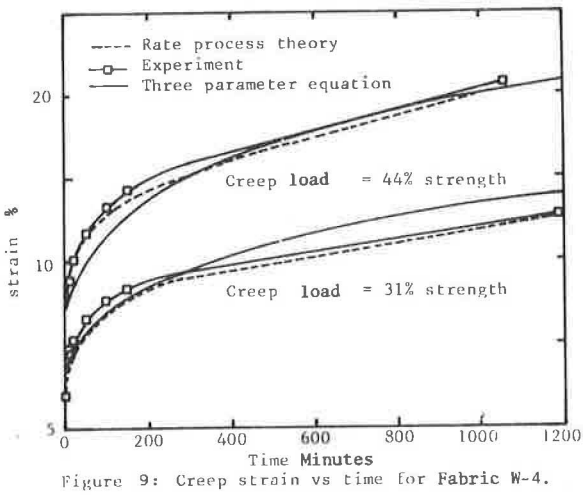

Figure 9: Creep strain vs time for Fabric W-4.

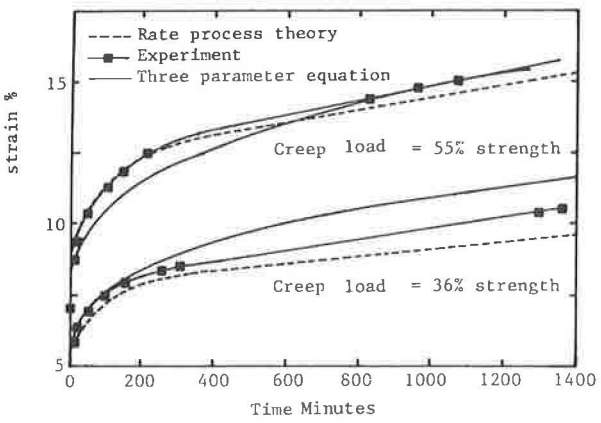

Figure 10: Creep strain vs time for Fabric C-1.

a comparison of the time estimated from the three-parameter creep equation and the Rate Process Theory for the geotextiles to creep to failure strains equal to those determined from wide strip tensile tests of the geotextile using specimens 200 mm (8 inches) wide and 100 mm (4 inches) initial gauge length.

Table 5. Estimated Time to Reach Ultimate Strain+ in a Creep Test

Fabric	ϵ_1* %	Ultimate+ Strain %	Load Level %	Time Required to Reach Ultimate Strain: Three-Parameter Equation	Time Required to Reach Ultimate Strain: Rate Process Theory
NW-1	4.0	23.0	40	485 days	22 days
NW-3	3.5	53	35	673 days	21 days
NW-5	23.0	98	37	107 days	19 days
NW-6	12.0	60	33	142 days	15 days
W-4	7.0	28	31	6 days	3 days
C-1	5.0	15	36	4 days	4 days

*ϵ_1 strain at time t = 1 minute

+ultimate strain measured by wide strip tensile test.

For the nonwoven geotextiles, the three-parameter creep equation predicted much longer times (142 to 485 days) than those predicted from the Rate Process Theory (15 to 22 days) for the failure strains to be reached by creep under sustained static loads. However, for the woven geotextiles both methods predicted creep times of the same order of magnitude.

The predicted time to reach failure strains under sustained loads are much shorter than the normal design lives of geotextile uses. There have been instances where geotextiles are known to resist static loads in the field without significant creep. For example, the first geotextile reinforced earth retaining wall designed by Bell (12) is performing satisfactorily without evidence of significant creep nearly a decade after its construction.

For both methods of creep characterization, determination of creep rate as a function of time is needed in order to develop the parameters. The creep strain rate was determined at any given time by measuring the slope of tangent to the experimental creep-time curve. Therefore, that the parameters determined by the Rate Process Theory and by the three-parameter creep equation are dependent upon the shape of the creep curve could introduce significant errors in the values of the creep constants. The results given in Tables 3 and 4 can best be considered as qualitative because of the limitation in the recording device used in the experiments. It was not possible to record the creep curve continuously for the full length of the experiment and the shape of the experimental creep curve was extrapolated after the first few hours to the observed creep strains at the end of the test (see Figures 5-10).

More important, however, may be the differences between the in-situ field conditions and the laboratory conditions. In the field the geotextile is confined by the soil while it is free in the laboratory strip tensile test. Also, field temperatures are usually much lower than the temperatures in the laboratory.

CONCLUSIONS

Creep-time curves predicted by the four-element rheological model based on Rate Process Theory appear to be more consistent with the experimental curves than those predicted by the three-parameter equation based on the empirical method.

Time to reach failure strains under sustained load predicted by the empirical method was much longer than the time predicted by the method based on Rate Process Theory for nonwoven geotextiles. However, for woven geotextiles, both methods predicted time to failure strains of the same order of magnitude.

Both methods predicted much shorter lives of geotextiles under sustained load than the normal design life of geotextile uses and shorter than indicated by actual field experience. This inconsistency needs further study with longer duration, more accurate tests which also consider temperature effects and simulate soil confinement.

ACKNOWLEDGEMENT

The authors gratefully acknowledge the financial support of the research reported in this paper by the United States Federal Highway Administration.

REFERENCES

(1). Al Hussaini, M.M., "Field Experiment of Fabric Reinforced Earth Wall," Proceedings, International Conference on the Use of Fabrics in Geotechnics, Vol. 1, Ecole Nationale Des Ponte et Chaussees, Paris, April 1977, pp. 119-122.

(2). Bell, J.R., Hicks, R.G., et al., "Test Methods and Use Criteria for Filter Fabrics," Interim Report Prepared for U.S. Department of Transportation, Federal Highway Administration, Oregon State University, Sept. 1978.

(3). Singh, A., Mitchell, J.K., "General Stress-Strain-Time Functions for Soils," Journal of the Soil Mechanics and Foundation Division, ASCE, SM1, Jan. 1968, pp. 21-46.

(4). Glasstone, S., Laidler, K., and Eyring, H., The Theory of Rate Process, McGraw-Hill Book Co., Inc., New York, 1941.

(5). Hogan, H.B., "The Engineering Application of the Absolute Rate Theory to Plastics: I - Laminates," Bulletin of the University of Utah, Vol. 42, No. 6, August 1951, pp. 1-147.

(6). Herrin, M. and Jones, G.E., "The Behavior of Bituminous Materials from the Viewpoint of the Absolute Rate Theory," Proceedings of the Association of Asphalt Paving Technologists, Vol. 32, Feb. 1963, pp. 82-105.

(7). Hady, M.A. and Herrin, M., "Characteristics of Soil-Asphalt as a Rate Process," Journal of the Highway Division, ASCE, HW1, March 1966, pp. 49-69.

(8). Christensen, R.W. and Wu, T.H., "Analysis of Clay Deformation as a Rate Process," Journal of Soil Mechanics and Foundation Division, ASCE SM6, November 1964, pp. 125-157.

(9). Mitchell, J.K., "Shearing Resistance of Soils as a Rate Process," Journal of the Soil Mechanics and Foundation Division, ASCE, SMT, January 1969, pp. 29-61.

(10). Mitchell, J.K., Campanella, R.G. and Singh, A., "Soil Creep as a Rate Process," Journal of the Soil Mechanics and Foundation Division, ASCE, January 1968, pp. 231-253.

(11). Coleman, B.D. and Knox, A.G., "The Interpretation of Creep Failure in Textile Fibers as a Rate Process," Textile Research Journal, May 1957, pp. 393-399.

(12). Bell, J.R. and Steward, J.E., "Construction and Observation of Fabric Retained Soil Walls," Proceedings, International Conference on the Use of Fabrics in Geotechnics, Vol. 1, Ecole Nationale Des Pontes et Chausses, Paris, April 1977, pp. 123-128.